0026-895X/06/7005-1503–1513
MOLECULAR PHARMACOLOGY
U.S. Government work not protected by U.S. copyright
Mol Pharmacol 70:1503–1513, 2006

Vol. 70, No. 5
26856/3145042
Printed in U.S.A.

A Three-Dimensional Quantitative Structure-Activity Relationship Study of the Inhibition of the ATPase Activity and the Strand Passing Catalytic Activity of Topoisomerase IIα by Substituted Purine Analogs[S]

Lars H. Jensen, Hong Liang, Robert Shoemaker, Morten Grauslund, Maxwell Sehested, and Brian B. Hasinoff

TopoTarget A/S, Copenhagen, Denmark (L.H.J., M.G.); Department of Pathology, Diagnostic Centre RH5431, Copenhagen University Hospital, Copenhagen, Denmark (L.H.J., M.S.); Developmental Therapeutics Program, National Cancer Institute at Frederick, Frederick, Maryland (R.S.); and Faculty of Pharmacy, University of Manitoba, Winnipeg, Manitoba, Canada (H.L., B.B.H.).

Received May 18, 2006; accepted July 31, 2006

ABSTRACT

Based on the topoisomerase IIα catalytic inhibitory activity of a previous hit compound, NSC35866, we screened 40 substituted purines or purine-like compounds from the National Cancer Institute repository for their ability to inhibit the ATPase activity of human topoisomerase IIα. Several compounds, including NSC348400, NSC348401 and NSC348402, were inhibitory at submicromolar concentrations. Three-dimensional quantitative structure-activity relationship models using comparative molecular field and comparative molecular similarity indices analyses were constructed using 24 of these compounds. The ability of 10 selected compounds to inhibit the complete DNA strand passage reaction of topoisomerase IIα correlated well with their potency as ATPase inhibitors. None of the 40 compounds significantly increased levels of the topoisomerase IIα-DNA covalent complex, suggesting that they functioned as catalytic topoisomerase II inhibitors and not as topoisomerase II poisons. Although some of these compounds could antagonize the effect of etoposide on the level of topoisomerase IIα-DNA covalent complex formation in vitro, in contrast to NSC35866, they were not capable of antagonizing etoposide-induced cytotoxicity and DNA strand breaks in cells. Two independently selected human SCLC cell lines with reduced topoisomerase IIα expression displayed cross-resistance to NSC348400, NBSC348401, and NSC348402, whereas an MDR1 line was fully sensitive. These results suggest that topoisomerase IIα is a functional cellular target for most of these substituted purine compounds and that these compounds do not display MDR1 liability.

Topoisomerase II is an essential nuclear enzyme found in all living cells. This enzyme transiently creates a protein-concealed double-strand break in one DNA molecule through which a second double-stranded DNA molecule can be transported (Wang, 2002). Topoisomerase II participates in various DNA metabolic processes, such as transcription, DNA replication, chromosome condensation, and de-condensation, and is essential at the time of chromosome segregation after cell division (Holm et al., 1985). Higher vertebrates have two isoforms, α and β, of this enzyme. Topoisomerase IIα is essential for cell proliferation and is most highly expressed in cells undergoing division (Akimitsu et al., 2003). The β isoform is not required for cell proliferation, but it is required for neural development (Yang et al., 2000).

Topoisomerase II-targeting drugs are among the most successful clinically applied anticancer compounds today and encompass such drugs as the epipodophyllotoxins (exemplified by etoposide and teniposide), the aminoacridines (exemplified by amsacrine), and the anthracyclines (exemplified by doxorubicin, daunorubicin, and idarubicin). These com-

This work was supported by the Canadian Institutes of Health Research, the Canada Research Chairs program, the Province of Manitoba, through the Manitoba Research and Innovation Fund and a Canada Research Chair in Drug Development (for B.H.) and by TopoTarget A/S.

Article, publication date, and citation information can be found at http://molpharm.aspetjournals.org.

doi:10.1124/mol.106.026856.

[S] The online version of this article (available at http://molpharm.aspetjournals.org) contains supplemental material.

ABBREVIATIONS: HPLC, high-pressure liquid chromatography; kDNA, kinetoplast DNA; 3D, three-dimensional; QSAR, quantitative structure-activity relationship; CoMFA, comparative molecular field analysis; CoMSIA, comparative molecular similarity index analysis; ICRF-187, dexrazoxane; ICRF-193, 4-((2*R*,3*S*)-3-(3,5-dioxopiperazin-1-yl)butan-2-yl)piperazine-2,6-dione; ICRF-154, 4-(2-(3,5-dioxopiperazin-1-yl)ethyl)piperazine-2,6-dione; F 11782, tafluposide.

pounds all belong to the "poison" class of topoisomerase II-directed drugs and work by a rather unusual mechanism in which they increase the levels of protein-concealed DNA double-strand breaks in cells (Wilstermann and Osheroff, 2003). The action of DNA metabolic processes then renders these complexes into permanent double-strand breaks, which are highly toxic to cells (Zhang et al., 1990). One general problem associated with topoisomerase II poisons is that they are toxic to several types of rapidly dividing cells in normal tissues, such as the bone marrow and the gut lining, which reduces their therapeutic index. The catalytic inhibitors constitute another class of topoisomerase II-interacting compounds that do not increase the levels of DNA breaks in cells at pharmacologically relevant concentrations. Several classes of structurally unrelated compounds including the bisdioxopiperazines [ICRF-187 (dexrazoxane), ICRF-193, and ICRF-154], the anthracycline derivative aclarubicin, the conjugated thiobarbituric acid-derived merbarone, the coumarin drugs novobiocin and coumermycin A1, the epipodophyllotoxin analog F 11782, fostrecin, and chloroquine all belong to this group, as has been extensively reviewed (Andoh and Ishida, 1998; Larsen et al., 2003). Combining a topoisomerase II poison with a catalytic topoisomerase II inhibitor (etoposide and ICRF-187) has been used to increase the therapeutic index of etoposide in a mouse central nervous system model of brain tumors (Holm et al., 1998). In addition, coadministration of etoposide and ICRF-187 has been found to be more effective than either agent alone in augmenting the effect of whole-brain irradiation in a mouse model (Hofland et al., 2005). These results pointed to the feasibility of using catalytic inhibitors as pharmacological modulators of topoisomerase II poisons, as suggested previously (Jensen and Sehested, 1997). In an attempt to identify novel structural entities targeting topoisomerase II as catalytic inhibitors, we previously identified NSC35866 as belonging to a new "purine class" of catalytic topoisomerase IIα inhibitors capable of antagonizing the effect of etoposide in vitro and in cells (Jensen et al., 2005). However, the potency of this compound against topoisomerase IIα was not high; hence, off-target effects might be expected. In the present communication, we report on the screening of 40 purine and purine-like compounds from the National Cancer Institute repository for the inhibition of the ATPase activity of topoisomerase IIα. Several compounds showed submicromolar inhibition of the ATPase activity of topoisomerase IIα as well as low micromolar activity against its complete DNA strand passage reaction, and they did this without increasing the level of topoisomerase IIα-DNA covalent complexes. These results establish these compounds as effective catalytic inhibitors of topoisomerase II. The purine compounds for which the stereochemistry was known were analyzed using 3D-QSAR modeling methods to identify the structural features responsible for their activity. Unlike NSC35866, the three most potent purines could not antagonize the effect of etoposide in cells, although they did so in vitro, suggesting that although they are catalytic topoisomerase IIα inhibitors, either they are not cell permeable enough or their interaction with topoisomerase IIα is different from that of NSC35866.

Materials and Methods

Materials and Cell Lines. The small-cell lung cancer cell lines OC-NYH, OC-NYH/DOX (topoisomerase IIα and IIβ down-regulated), OC-NYH/DAU (MDR1 overexpression), OC-NYH/VM (topoisomerase IIα down-regulated), and OC-NYH/pACR8 (topoisomerase IIβ down-regulated) (Rothenborg-Jensen et al., 2001), human ovary cancer A2780 cells, human prostate cancer PC3 cells, and colon cancer HTC116 cells have been described previously and are all well characterized cell lines. All cells were grown in RPMI 1640 medium supplemented with 10% fetal calf serum and 100 U/ml penicillin-streptomycin at 37°C in atmospheric air supplemented with 5% CO_2. The hydrochloride salt of ICRF-187 [dexrazoxane (Cardioxane); Chiron Group, Emeryville, CA) was dissolved in sterile water. Etoposide was purchased from Bristol-Myers Squibb (Lyngby, Denmark) and was dissolved in sterile water. The purine and purine-like compounds were supplied by the Drug Synthesis and Chemistry Branch, Development Therapeutics Program, Division of Cancer Treatment and Diagnosis, National Cancer Institute (Bethesda, MD), and dissolved in dimethyl sulfoxide at concentrations ranging from 10 to 100 mM. [^{3}H]dATP, [^{3}H]thymidine, and [^{14}C]thymidine were purchased from GE Healthcare (Little Chalfont, Buckinghamshire, UK). All other compounds were purchased from Sigma-Aldrich (Brondby, Denmark) and were dissolved in dimethyl sulfoxide. The structure of the template compound NSC348400[1] and of all the substituted purines or purine-like analogs used in this study can be found in Fig. 1 and supplementary Fig. S1, respectively.

Identification and Purity of Representative Purine Analogs. The identity and chromatographic purity of a representative subset of the purine compounds obtained from the National Cancer Institute were determined by high-pressure liquid chromatography (HPLC)/UV-mass spectrometry. The HPLC apparatus consisted of an Alliance Separation Module 2795 (Waters, Milford, MA) connected to a Waters 2996 Photodiode Array Detector and a Quattro Premier Tandem Mass Spectrometer (Waters-Micromass, Manchester, UK) with the electrospray interface used in positive ion mode. Data were acquired and processed with MassLynx version 4.1 software. The chromatographic purity was calculated from the percentage peak area that the mass spectrometric-identified purine compound was of the total of all observed peak areas. Six of the purine compounds (NSC19865, NSC35866, NSC348400, NSC348401, NSC348402, and NSC39055) were selected for comprehensive HPLC diode array detection/electrospray mass spectrometry analysis to both identify and to obtain purity data on a subset of the purine compounds as representative of the larger set. Mass spectrometric analysis positively confirmed the identity of all of the compounds selected for analysis. The HPLC-determined chromatographic purity values found were 99.8, 99.7, 92.6, 88.2, 86.0, and 82.7% for NSC19865, NSC35866, NSC348400, NSC348401, NSC348402, and NSC39055, respectively.

Purification of Human Topoisomerase IIα from Overexpressing Yeast Cells. Full-length human wild-type and mutant topoisomerase IIα was purified from overexpressing yeast cells as described previously (Rothenborg-Jensen et al., 2001) to greater than 95% purity as judged by SDS-polyacrylamide gel electrophoresis and Coomassie blue staining.

ATPase Assay. The ATP hydrolysis catalyzed by topoisomerase IIα was studied with a linked kinetic enzyme assay (Lindsley, 2001) and, as described previously (Jensen et al., 2005), by following the oxidation of NADH at 340 nm on a Bio-Tek EL808 Ultra Micro plate Reader connected to a PC with KC4 software (Bio-Tek Instruments, Winooski, VT). Reactions were performed in 96-well plates (Microtest 96-well Clear Plate; BD Biosciences, San Jose, CA) at 37°C in a total volume of 400 μl. The reaction contained 18 nM topoisomerase IIα and 1 mM ATP. As described previously (Jensen et al., 2005), closed circular 18.5-kbp DNA was added to obtain a DNA base pair to enzyme-dimer ratio of 850:1. In general, the percentage remaining

[1] The structures and names of all the National Cancer Institute NSC numbered compounds used in this study may be found at the following website: http://129.43.27.140/ncidb2/.

ATPase activity of 6 to 10 replicates was measured at each drug concentration.

The IC_{50} values for the inhibition of the ATPase activity of topoisomerase IIα were determined by nonlinear least-squares fitting (SigmaPlot; Systat Software, Point Richmond, CA) of f, the fractional remaining activity, as a function of the inhibitor concentration to a two-parameter sigmoidal equation $f = (1 - d)/(1 + ([\text{drug}]/IC_{50})^{n_H}) + d$, where IC_{50} and n_H, the Hill coefficient, were the best fit parameters, and d was the limiting fractional remaining activity observed at the highest inhibitor concentration used.

DNA Strand Passage Assay. Topoisomerase IIα catalytic activity (DNA strand passage activity) was measured using a filter-based kDNA decatenation assay using *Crithidia fasciculata* ^{3}H-labeled kDNA as described previously (Jensen et al., 2002). The IC_{50} values for the percentage inhibition of topoisomerase IIα was obtained by nonlinear least-squares fitting of the percentage inhibition data to a two-parameter sigmoidal equation as a function of the inhibitor concentration: % inhibition = $(100)/(1 + (IC_{50}/[\text{drug}])^{n_H})$, where IC_{50} and n_H were the best fit parameters.

Topoisomerase IIα-DNA Covalent Complex Formation Assay. The level of topoisomerase IIα-DNA covalent complex formation was assessed using a new and highly sensitive assay based on phenol-chloroform extraction as described previously (Jensen et al., 2005). In brief, a 950-base pair linear ^{3}H-labeled DNA was synthesized by the polymerase chain reaction in the presence of [^{3}H]dATP. The DNA fragment was isolated from unincorporated deoxynucleotide triphosphates by gel filtration followed by ethanol precipitation. The 50-μl reaction mixtures containing 100 ng of radiolabeled DNA fragment, 300 to 700 ng of topoisomerase IIα, topoisomerase II cleavage buffer (10 mM Tris-HCl, pH 7.9, 50 mM NaCl, 50 mM KCl, 5 mM $MgCl_2$, 1 mM EDTA, 15 μg/ml bovine serum albumin, and 1 mM Na_2ATP), and increasing concentrations of drug were incubated for 30 min at 37°C. A "no topoisomerase IIα" sample was always included for normalization purposes. The cleavable complex was trapped by adding 5 μl of 10% SDS. After vigorous vortexing for 30 s, 45 μl of Tris-EDTA buffer, pH 8.0, was added to obtain 100 μl per sample. A 100-μl volume of phenol/chloroform/isoamyl alcohol [25:24:1 (v/v/v)] equilibrated with Tris-EDTA buffer, pH 8.0, was then added, and the samples were vortexed vigorously for 30 s. The samples were finally centrifuged at 20,000*g* for 2 min, and 90 μl of the upper water phase was used for scintillation counting using 15 ml of Ultima gold scintillation fluid (PerkinElmer Life and Analytical Sciences, Boston, MA).

Clonogenic Assay. The assay was performed as described previously (Jensen et al., 1993).

Alkaline Elution Assay. The alkaline elution assay was performed as described by Kohn and Grimek-Ewig (1973) with the modifications described previously (Sehested et al., 1993).

Modeling and Conformation Search. All molecular modeling was done using SYBYL 7.1 (Tripos, St. Louis, MO) on a Hewlett-Packard XW4100 PC workstation with a Redhat Enterprise 3 Linux operating system. All molecules were built using SYBYL. All molecules were first geometry-optimized with the Tripos force field using a conjugate gradient with a convergence criterion of 0.01 kcal/mol, Gasteiger-Huckel charges, and a distance-dependent dielectric constant. The SYBYL CONFORT module was then used to find the lowest energy conformation.

3D-QSAR Analyses. The CoMFA and CoMSIA analyses require that the 3D structures of the molecules be aligned to a core conformational template that is their presumed active form (Cramer III et al., 1988; Klebe et al., 1994; Kubinyi et al., 1998). The second most active compound, NSC348400, was chosen as the template molecule to ensure a large enough grid in the space occupied by its sugar residue. The five common core bonds to which all the molecules were aligned for the 3D-QSAR analyses are shown in bold red in Fig. 1A, and the actual alignments are depicted in Fig. 1B. The molecular conformations that were used for alignment were the conformers that had the lowest energy obtained with the SYBYL CONFORT module after performing a global minimization search. For the CoMFA analysis, steric and electrostatic field energies were calculated using an sp^3 carbon with a van der Waals' radius of 1.52 Å as the steric probe and a +1 charge as an electrostatic probe. Steric and electrostatic interactions were calculated using the Tripos force field with a distance-dependent dielectric constant at all lattice points of a regular spaced (2 Å) grid. The energy cutoff was 30 kcal/mol. The alignment and lattice box used for the CoMFA calculation were also used to calculate similarity index fields for the CoMSIA analysis. Steric, electrostatic, hydrophobic, hydrogen bond donor, and acceptor fields were evaluated in the CoMSIA analysis. Similarity indices were computed using a probe atom with +1 charge, radius 1 Å, hydrophobicity +1, hydrogen bond donating +1, hydrogen bond acceptor +1, and attenuation factor α 0.3 for the Gaussian-type distance. A partial least-squares statistical approach, which is an extension of multiple regression analysis in which the original variables are replaced by a set of their linear combinations, was used to obtain the 3D-QSAR results. All models were investigated using

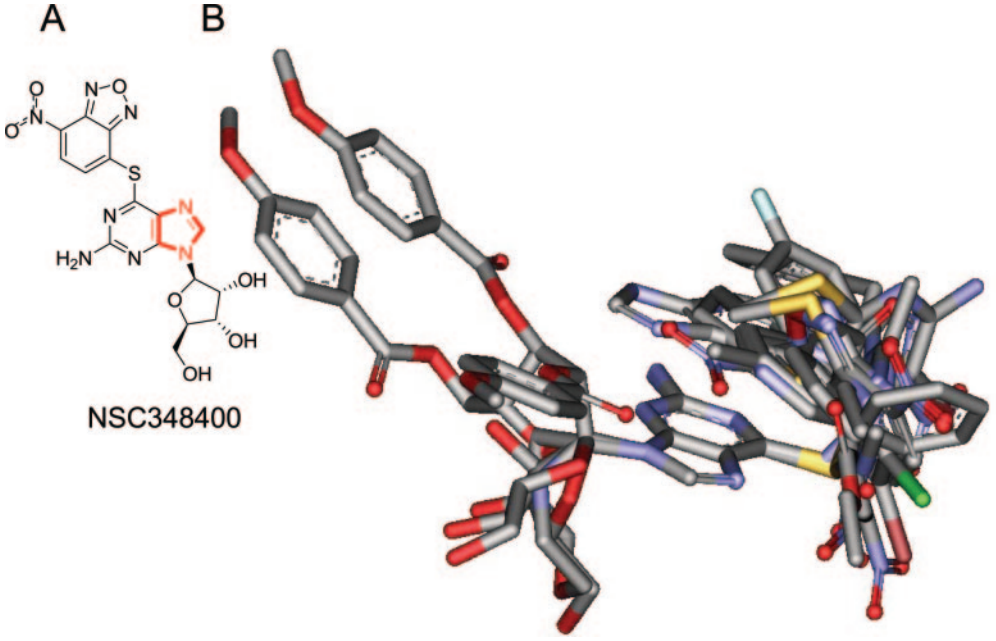

Fig. 1. A, structure of NSC348400 purine used as a template molecule in 3D-QSAR modeling. The five-membered ring structure used for molecular alignments is represented in bold red. B, structures of 25 purine and purine-like energy-minimized structures aligned to the template molecule NSC348400 used in the 3D-QSAR modeling.

the leave-one-out method, which is a cross-validated partial least-squares method. The CoMFA and CoMSIA descriptors were used as independent variables and pIC_{50} ($-\log IC_{50}$, in molar concentration units) was used as the dependent variable to derive the 3D-QSAR models. The q^2 (cross-validated correlation coefficient r^2) and the optimum number of components (N) were obtained by the leave-one-out method. The final model (non–cross-validated conventional analysis) was developed and yielded the non–cross-validated correlation coefficient r^2 with the optimum number of components.

Results

Inhibition of Topoisomerase IIα ATPase Activity by The Purine and Purine-Like Compounds. We previously reported that NSC35866, an S^6-substituted purine, inhibited the ATPase and DNA strand passage activity of topoisomerase IIα without generating DNA damage in vitro and in vivo (Jensen et al., 2005). The inhibitory activity of this lead compound was low, however, with IC_{50} values of 30 μM in the ATPase assay and 750 μM in the DNA strand passage assay. To identify more potent inhibitors of the ATPase activity of topoisomerase IIα, we screened 40 substituted purine or purine-like compounds that we identified in the National Cancer Institute repository. Some compounds were selected on the basis of structural similarity with the lead purine NSC35866 (Jensen et al., 2005), and others were selected by mining the National Cancer Institute 3D-MIND database for compounds having cytotoxicity profiles similar to that of the most potent compound NSC348401 as assessed by the National Cancer Institute using their 60-cell line cancer screen. Some compounds belonging to the latter group were purine-containing Hg^{2+} and Pd^{2+} metal complexes, and a few other compounds contained only the imidazole part of the purine ring structure. The structures of all compounds screened in the ATPase assay are depicted in supplementary Fig. S1. After carrying out initial pilot experiments to assess the relative potency of these compounds as inhibitors of the ATPase reaction of topoisomerase IIα, the inhibitory effect of all compounds was tested at five different drug concentrations depending on the potency of the individual compound. Within each experiment, the rate of ATP hydrolysis observed in the absence of drug was set to one. Some of the least active compounds were tested at only four concentrations as a result of limited solubility. All of the primary screening data that were obtained are shown in supplementary Fig. S2. Even the most potent compounds at the highest concentrations inhibited the topoisomerase IIα ATPase activity only

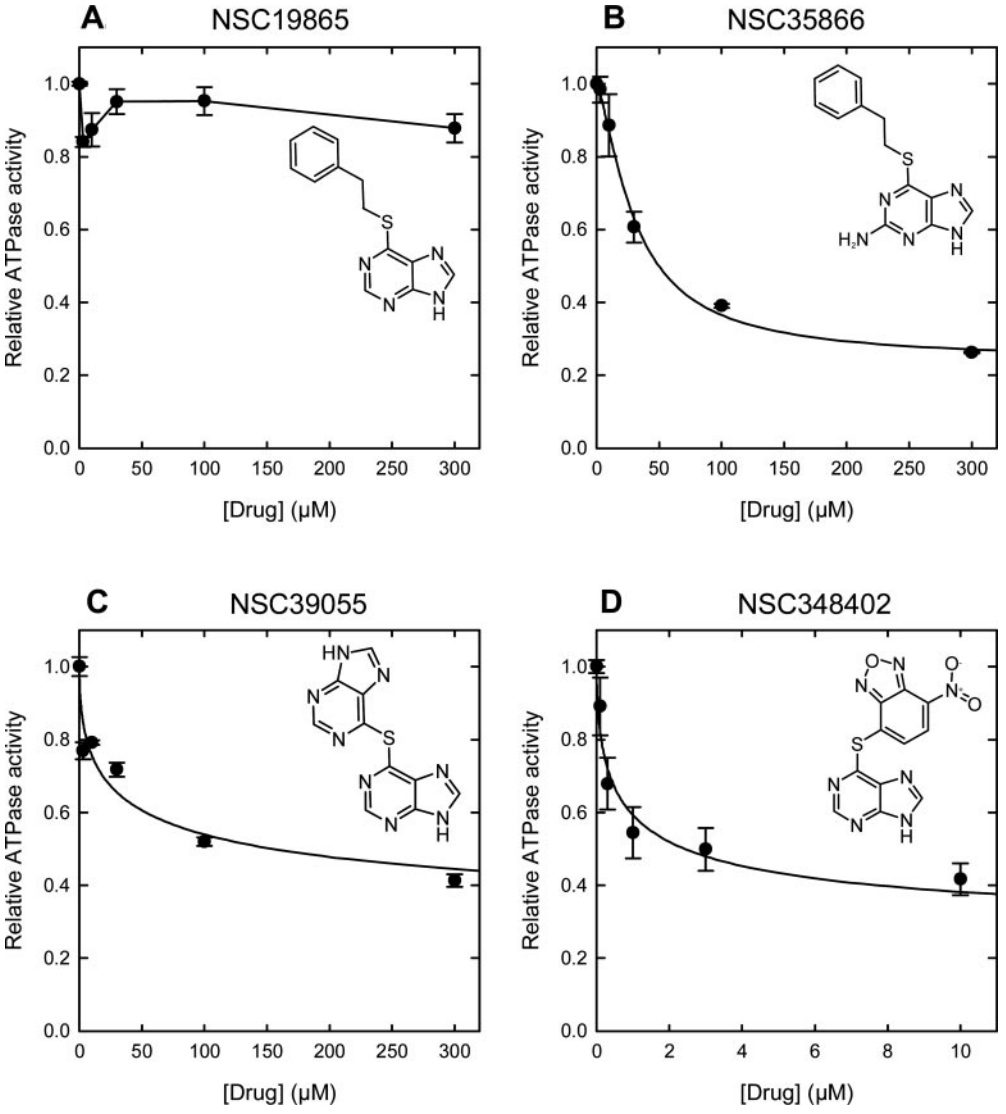

Fig. 2. Representative examples for the inhibition of the ATPase activity of topoisomerase IIα by some purine compounds. A, B, C, D, effect of increasing concentrations of NSC19865, NSC35866, NSC39055, and NSC348402, respectively, on the rate of ATP hydrolysis by topoisomerase IIα in the presence of DNA. Error bars represent S.E.M. of 2 to 10 determinations. The curved solid lines are from nonlinear least-squares fits to the equation described under *Materials and Methods*.

down to 24% residual remaining activity. The inhibition data were not suggestive of competitive inhibition because only partial inhibition of the ATPase activity was achieved, even at the highest inhibitor concentrations used (Fig. 2 and supplementary Fig. S2). This mode of inhibition was similar to that seen for catalytic inhibition of topoisomerase II by ICRF-193, which is not a competitive inhibitor of topoisomerase II ATPase activity in the presence of DNA (Morris et al., 2000). Thus, the value of d, which is the fractional remaining activity that was observed using the most potent inhibitor at the highest inhibitor concentrations used, was fixed at a value of 0.24 in the two-parameter sigmoidal fitting equation described under *Materials and Methods* to obtain an empirical IC_{50} value that could be used in the 3D-QSAR analysis. The result of this analysis yielded IC_{50} values ranging from 0.05 to 2100 μM, which is a range of more than 10,000-fold. When the heavy metal-complexes were excluded, the IC_{50} values observed were in the range of 0.4 to 2100 μM, which still represented a greater than 1000-fold difference. The calculated IC_{50} values for all 40 compounds are presented in supplementary Table S1. A few examples from this analysis in which relatively minor changes in compound structure resulted in pronounced changes in potency as ATPase inhibitors are shown in Fig. 2. The substitution of an amino group at position C2 in two otherwise identical molecules (compare NSC 19865 in Fig. 2A and NSC35866 in Fig. 2B) resulted in inhibition of the topoisomerase IIα ATPase activity going from >300 μM to 31 μM. Likewise, the relatively small changes seen between NSC39055 and NSC348402 (Fig. 1, C and D, respectively) resulted in an increase in potency of more than 100-fold.

Construction of 3D-QSAR Models Based on the Inhibition of the ATPase Activity of Topoisomerase IIα. The wide range of ATPase IC_{50} values allowed us to carry out 3D-QSAR CoMFA and CoMSIA analyses to identify the structural features responsible for the inhibitory activity of the purine compounds. The results of the CoMFA and CoMSIA analyses of the pIC_{50} data (Table 1) for the inhibition of the ATPase activity of topoisomerase IIα are summarized in Table 2. The purine analogs that were complexes of either Hg^{2+} or Pd^{2+} (a member of the platinum group metals) were not included in the data set used because it is well known that these heavy metal ions have a very high affinity for thiol groups on proteins that typically lead to their inactivation. Thus, they are likely to nonspecifically inhibit topoisomerase IIα activity, as we have shown for cisplatin (Hasinoff et al., 2005) and has been shown for Co^{2+} (Baldwin et al., 2004) and selenium-containing compounds (Zhou et al., 2003). Several other studies have shown that sulfhydryl-reactive compounds, including maleimide (Jensen et al., 2002) and a variety of quinones (Wang et al., 2001; Hasinoff et al., 2006), also inhibit topoisomerase II. Compounds with an unknown *Z*/*E* and/or unknown *R* or *S* stereochemical configuration, or compounds with C=C, C=N, and N=N double bonds (NSC36824, NSC45388, NSC684046, NSC75140, NSC83112) were also not included in the data set because the CoMFA and CoMSIA analyses require that the absolute structures be known. NSC46384 and NSC29421 were found to be single outliers in the CoMFA and CoMSIA analyses, respectively, and were likewise omitted. Because of the relatively small numbers of compounds in each data set (24), all structures were used in the analyses rather than dividing them into training and validation sets. The predicted and experimental pIC_{50} values are plotted in Fig. 3. For both the CoMFA and CoMSIA analyses, the predicted and experimental pIC_{50} values were well correlated with r^2 values of 0.936 and 0.825, respectively. Furthermore, the CoMFA and CoMSIA analyses of the IC_{50} data gave high q^2 values (0.610 and 0.660, respectively; Table 2), indicating that the model and the alignments used were good predictors of the activity.

The steric and electrostatic contributions (49.9% and 50.1%, respectively) to the CoMFA field were almost the same (Table 2). The CoMSIA analysis, in addition to the steric and electrostatic contributions to the field, also measures hydrophobic and hydrogen bond donor and acceptor contributions to the field. The hydrophobic contribution to

TABLE 1
Experimental pIC_{50} values and residuals from the calculated values obtained from CoMFA and CoMSIA 3D-QSAR analysis for the inhibition of the ATPase activity of topoisomerase IIα

NSC No.	pIC_{50}	Residuals[a]	
		CoMFA	CoMSIA
	M		
15747	4.87	0.55	0.56
29421	2.89	−0.55	Outlier
35862	4.07	−0.02	−0.14
35865	4.27	−0.05	−0.03
35866	4.51	−0.15	0.24
38732	4.47	−0.07	−0.40
39055	4.37	0.07	−0.05
39328	3.82	−0.41	−0.45
39330	3.68	0.17	−0.48
39331	4.72	0.04	0.26
40818	3.89	0.11	−0.20
42375	5.10	0.28	0.21
46384	4.85	Outlier	0.65
48388	3.84	−0.03	−0.38
52383	4.90	0.16	0.46
52388	4.44	−0.01	0.09
71261	4.80	−0.05	0.31
76519	4.88	0.03	0.36
133593	3.71	0.21	−0.47
172614	3.92	−0.28	−0.33
244708	5.56	0.18	0.22
348400	6.41	0.01	−0.20
348401	6.43	−0.06	0.09
348402	6.11	−0.20	−0.14
647471	3.93	0.06	−0.17

[a] Observed – predicted values.

TABLE 2
Partial least-squares statistics and field contributions from CoMFA and CoMSIA models for the prediction of pIC_{50} for the inhibition of the ATPase activity of human topoisomerase IIα

Parameter	CoMFA	CoMSIA
PLS statistics		
q^2	0.610	0.660
N	3	1
S.E.P.	0.593	0.483
r^2	0.936	0.825
S.E.E.	0.240	0.346
F	97	104
Field contributions		
Steric	0.499	0.073
Electrostatic	0.501	0.156
Hydrophobic		0.498
Hydrogen bond donor		0.205
Hydrogen bond acceptor		0.067

q^2, leave-one-out (LOO) cross-validated correlation coefficient, N, optimum number of components; S.E.P., standard error of prediction; r^2, non–cross-validated correlation coefficient; S.E.E., standard error of the estimate; F, F-test value.

the CoMSIA-derived field, at 49.8%, was the largest contributor to the overall field (Table 2). The hydrogen bond donor and electrostatic components at 20.5% and 15.6%, respectively, were the second and third largest contributors to the field (Table 2).

The isocontour diagrams ("stdev*coeff," Figs. 4 and 5) that were mapped onto the NSC348400 template molecule of Fig. 1A as described under *Materials and Methods* show the regions in space that were either favored or disfavored for inhibitory activity. The green contours indicate regions that increased inhibitory activity, and the red contours indicate regions that decreased inhibitory activity. The steric isocontours gave similar results for both the CoMFA and CoMSIA analyses (Fig. 4, compare A and B). These steric fields favored the planar phenyl group as found in NSC348400 and in many of the other analogs. The steric fields disfavored a linker methylene group bonded to the sulfur ether atom. An examination of these compounds using stereo glasses showed that purine analogs with this linker methylene group connected to the phenyl ring were able to bend over and become nearly coplanar with the purine ring. As shown in Fig. 4D, the electrostatic field for the CoMSIA analysis was more localized than for the CoMFA analysis depicted in Fig. 4C. The polar nitro groups and the polar benzoxadiazol group as in NSC348400 were highly favored. Therefore, polar substitutions in this area should lead to more active compounds.

The hydrophobic field depicted in Fig. 5A makes the largest contribution to the CoMSIA-derived field. There is a large green favored area around the phenyl group that is directly bonded to the sulfur ether atom as in NSC348400. This is a common substitution in a number of the highly active analogs. This result suggests that even larger more hydrophobic groups might be accommodated in this area to produce more active compounds. There was no significant red disfavored hydrophobic field seen in the CoMSIA analysis.

The second largest contribution to the CoMSIA-derived field was the hydrogen bond donor field shown in Fig. 5B. The largest area that was disfavored was in the vicinity of the ribose sugar substituted to the purine ring. Thus, the hydrogen bond donor atoms on the sugar do not contribute positively to the inhibitory activity of these compounds. This result can be partly explained by a comparison of the structures of NSC348400, NSC348401, and NSC348402. Although NSC348400 contains a sugar group, the latter two compounds that were of equal potency do not, and thus a sugar group is not favored in this position. There were also two positive contributions to the hydrogen bond donor field in the area around each of the hydrogen atoms of the amino group substituted on the purine ring as in NSC348400, indicating the importance of the 2-amino group for the activity.

Potency of Selected Purine Analogs As Inhibitors of Topoisomerase IIα DNA Strand Passage Coincides with Their Potency As ATPase Inhibitors. To determine whether the potency of the purine and purine-like compounds, as determined in the ATPase assay, was correlated with their potency as inhibitors of the full DNA strand passage reaction of topoisomerase II, we assessed the effect of 10 selected purine compounds on topoisomerase IIα decatenation activity using a filter-based assay described previously (Jensen et al., 2002) using a known catalytic topoisomerase IIα inhibitor, ICRF-187, as a positive control. This assay measures radioactively labeled kDNA substrate left on the filter after filtering and washing. Therefore, high counts represent inhibition of topoisomerase IIα decatenation activity. In this analysis, the number of counts per minute derived from all "no drug" samples were averaged, and this value was normalized to 0% inhibition. In a similar fashion, all the numbers of counts per minute from the "no enzyme" reactions were averaged, and this value was normalized to 100% inhibition. The results of these analyses are shown in Fig. 6. Figure 6A depicts results obtained with a group of purine compounds of lower potency in the ATPase assay, whereas Fig. 6B depicts results obtained with compounds of higher potency. As shown in Fig. 6C, the inhibition of the topoisomerase IIα decatenation activity was well correlated (r^2 of 0.88) with the ATPase inhibitory activity. Furthermore, the slope of the log-log plot of 0.89 ± 0.13 was 1 within 1 S.E.M. Several compounds, including the nonmetal containing analog NSC348400, are even more effective inhibitors than the positive control ICRF-187. Together, these results suggest that inhibition of ATPase activity was a good predictor for inhibition of the intact DNA strand passage activity for these purine analogs.

Lack of Stimulation of Topoisomerase IIα-DNA Covalent Complexes by Purine Analogs. Compounds that target topoisomerase II can be divided into two major classes: 1) topoisomerase II poisons that increase the levels of topoisomerase II-DNA covalent complexes and 2) catalytic inhib-

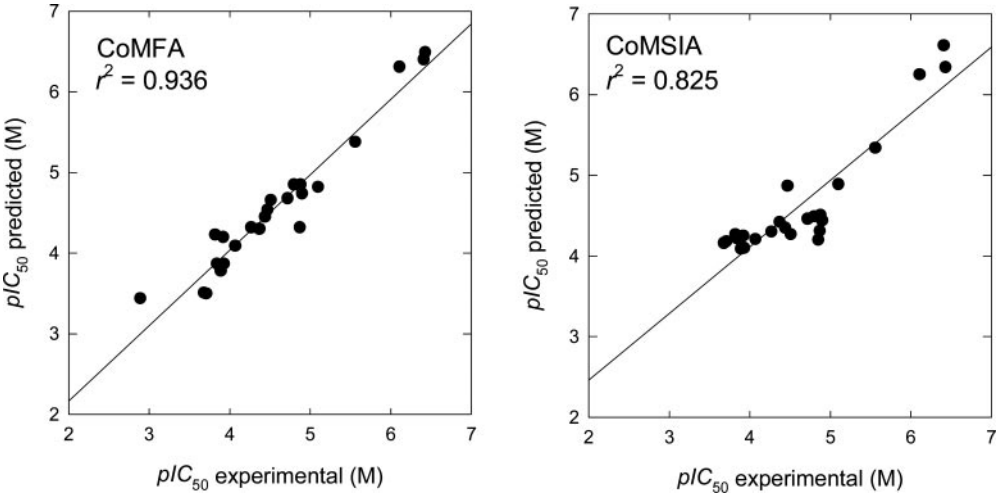

Fig. 3. Correlation between the predicted and experimentally determined values of pIC_{50} for inhibition of the ATPase activity of topoisomerase IIα by the 24 purine analogs used in the building of the CoMFA (left) and CoMSIA (right) models.

itors that do not increase the levels of this complex. Both classes are known to interfere with the ATPase and DNA strand passage activity of topoisomerase II. We therefore probed the effect of all purine compounds on the level of this complex produced in vitro by using a highly sensitive assay described previously (Jensen et al., 2005). To gain the highest possible sensitivity, this assay was performed at a very high topoisomerase IIα-to-DNA ratio of 700 ng of topoisomerase IIα per 100 ng of DNA. Under these conditions, approximately half the DNA was trapped as covalent complex in the absence of any drug, and thus even a small increase in the level of this complex was easily detected. The result of this analysis is depicted in supplementary Fig. S3. Of the 40 compounds analyzed, only the Hg^{2+}-containing NSC321239 increased the level of covalent complexes to any significant extent. Together, these results confirm that, in general, the purine analogs are catalytic inhibitors of topoisomerase II and are not topoisomerase IIα poisons.

Antagonism of Etoposide-Induced DNA-Topoisomerase IIα Covalent Complex Stimulation by the Three Most Potent Nonmetal Purine Analogs. We have shown previously that catalytic topoisomerase II inhibitors have the capacity to antagonize the effect of the nonintercalating topoisomerase II poison etoposide (Sehested and Jensen, 1996). We therefore assessed whether three of the most active compounds (NSC348400, NSC348401, and NSC348402) were capable of antagonizing the ability of etoposide to promote topoisomerase IIα-DNA covalent complexes in vitro. We assessed this by using the same assay described above, but this time we used a topoisomerase IIα-to-DNA weight ratio of 3 to 1 instead of 7 to 1. The results of these analyses are depicted in Fig. 7A for NSC348400 and Fig. 7B for NSC348402. In the absence of drug, the level of covalent complex was approximately 20% (represented by the dotted line in both panels). In the presence of 1 μM etoposide, this value was increased by approximately 50%. Increasing concentrations of NSC348400 or NSC348402 clearly antagonized the effect of etoposide in a dose-dependent manner. At concentrations of 10 μM and above, both compounds completely abolished the effect of etoposide. Similar results were obtained for NSC348401 (data not shown).

Lack of Protection of Etoposide-Induced Cytotoxicity and DNA Strand Breaks in Cells by the Most Potent Nonmetal Purine Analogs. We previously showed that NSC35866 is capable of antagonizing the cytotoxicity of etoposide in human cancer cells. Using an assay with 20 min of preincubation with NSC35866, followed by a 1-h coincubation with etoposide, up to 50-fold protection was observed (Jensen et al., 2005). We therefore tested whether the three most potent nonmetal analogs (NSC348400, NSC348401, and NSC348402) could antagonize the 1-h cytotoxicity induced by etoposide and daunorubicin with small-cell lung cancer OC-NYH, ovary cancer A2780, prostate cancer PC3, and colon cancer HTC116 human cancer cell lines. However, in contrast to NSC35866, these three potent compounds were not effective antagonists of topoisomerase II poison-induced cytotoxicity (data not shown). Furthermore, when assessed in an alkaline elution assay, NSC348401 had no effect on the level of etoposide-induced DNA strand breaks (data not shown), unlike NSC35866, which was previously found to antagonize such breaks (Jensen et al., 2005).

The Purine Analogs Are Not Cross-Resistant to Two Mutant Topoisomerase IIα Enzymes That Are Highly Cross-Resistant to ICRF-187 and ICRF-193. We have previously characterized mutations in the bisdioxopiperazine binding site of topoisomerase IIα that lead to a high degree of cross-resistance to inhibition by ICRF-187 and ICRF-193 (Wessel et al., 2002). The Tyr50Phe and Tyr165Ser mutations in human topoisomerase IIα provide a means by which we can test whether the purine analogs bind to the bisdioxopiperazine binding site, which has been identified by X-ray crystallography to span the dimer interface in the N-terminal region close to the ATP binding sites (Classen et al., 2003).

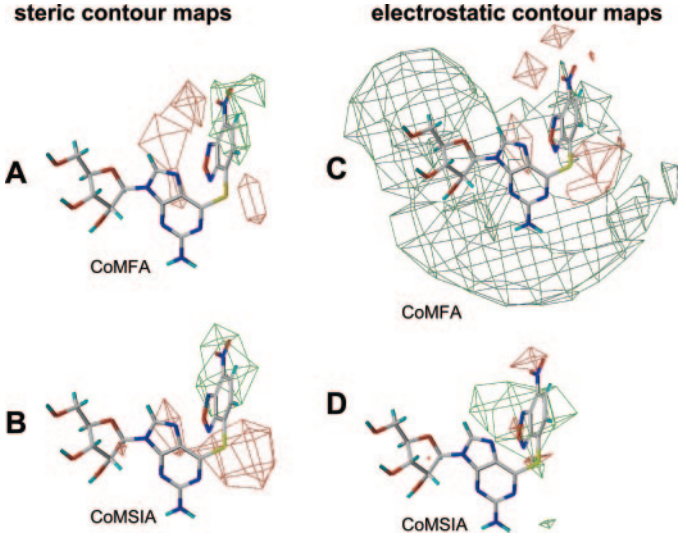

Fig. 4. Steric and electrostatic contour maps superimposed on the structure of NSC348400 obtained from the CoMFA (A and C) and CoMSIA (B and D) modeling, respectively, for the inhibition of the ATPase activity of topoisomerase IIα by 24 purine analogs. The green grids outline the regions in space that are favored for inhibition of the ATPase activity of topoisomerase IIα, and the red areas show the regions that are disfavored.

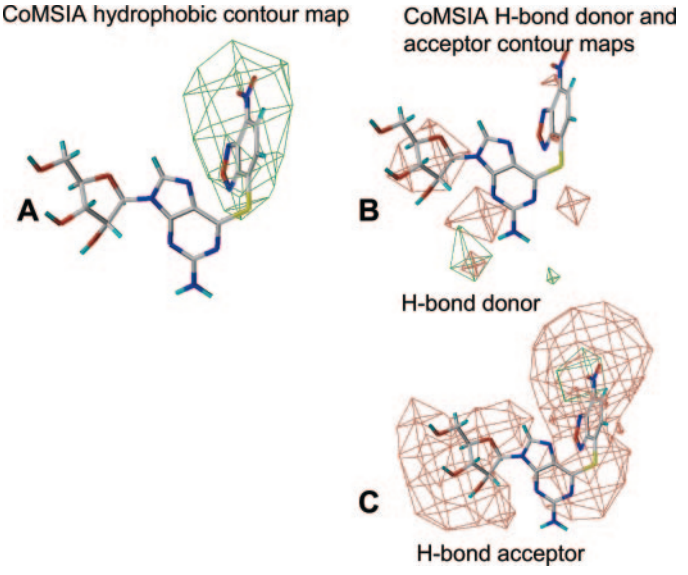

Fig. 5. Hydrophobic (A), H-bond donor (B), and H-bond acceptor (C) contour maps superimposed on the structure of NSC348400 obtained from the CoMSIA 3D-QSAR modeling for the inhibition of the ATPase activity of topoisomerase IIα by the 24 purine analogs. The green grids outline the regions in space that are favored for inhibition of the ATPase activity of topoisomerase IIα, and the red areas show the regions that are disfavored.

We have measured IC_{50} values for inhibition of decatenation on four of the purine analogs (NSC19865, NSC348400, NSC348401, and NSC348402) using purified wild-type and ICRF-187-resistant mutant topoisomerase IIα (Wessel et al., 2002). Relative resistance ratio values for the Tyr50Phe mutant topoisomerase IIα compared with wild-type enzyme were 0.19, 0.25, 0.20, and 0.25 for NSC19865, NSC348400, NSC348401, and NSC348402, respectively. Likewise, relative resistance ratio values for the Tyr165Ser mutant topoisomerase IIα compared with wild-type enzyme were 0.20, 0.41, 0.24, and 0.20 for NSC19865, NSC348400, NSC348401, and NSC348402, respectively. Thus, none of these purine analogs displayed cross-resistance and all were in fact slightly hypersensitive. These results suggested that the purine analogs did not inhibit topoisomerase IIα by binding to the bisdioxopiperazine binding site. The reason for the hy-

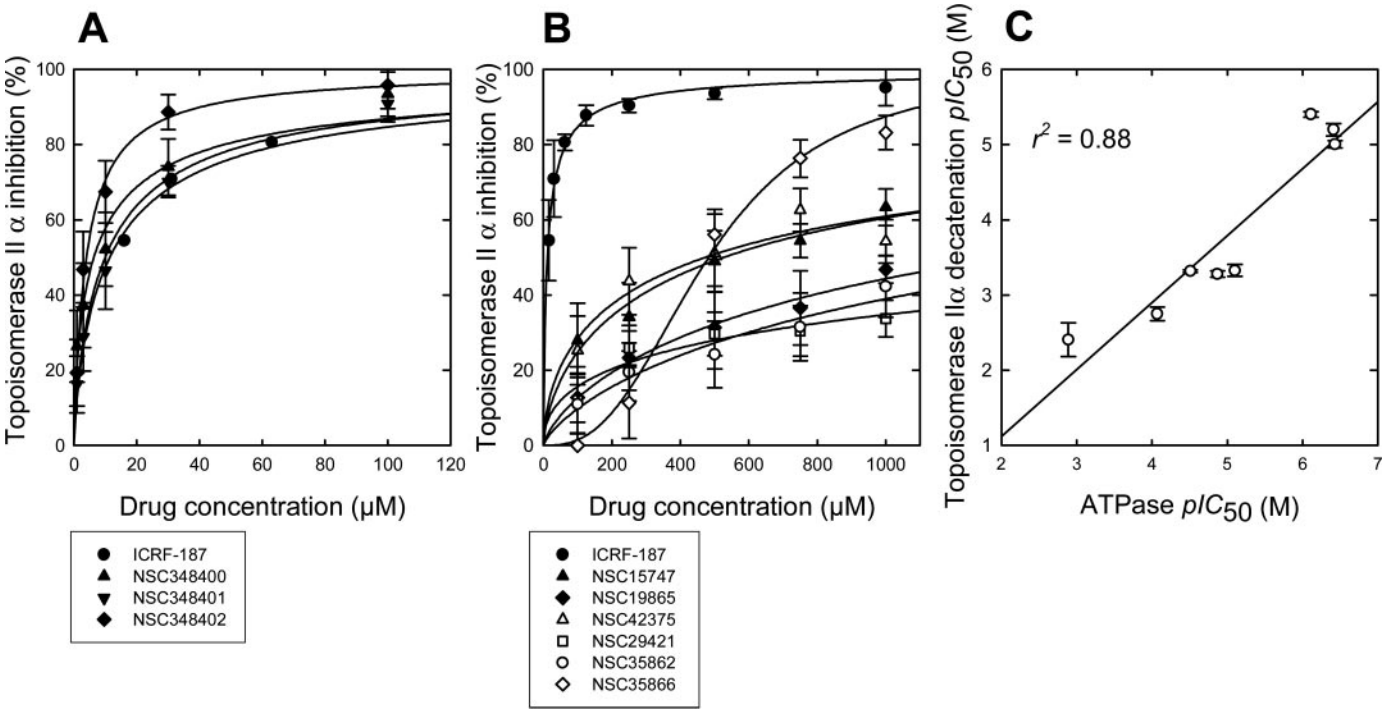

Fig. 6. Inhibition of the DNA strand passage reaction of topoisomerase IIα by 10 selected purine analogs and their correlation with their inhibition of the ATPase activity of topoisomerase IIα. A, inhibition by three potent purine compounds and ICRF-187 for comparison. B, inhibition by six of the less potent purine compounds and ICRF-187 for comparison. Error bars represent S.E.M. of three independent experiments. The curved lines were obtained using nonlinear least-squares fits of the data to the equation described under *Materials and Methods*. C, correlation of the pIC_{50} ($-\log IC_{50}$, in molar concentration units) for the inhibition of the strand passage (decatenation) of kDNA by topoisomerase IIα with the ATPase activity of topoisomerase IIα. The straight line was least-squares–calculated and has a slope of 1 within the S.E.M. of its determination.

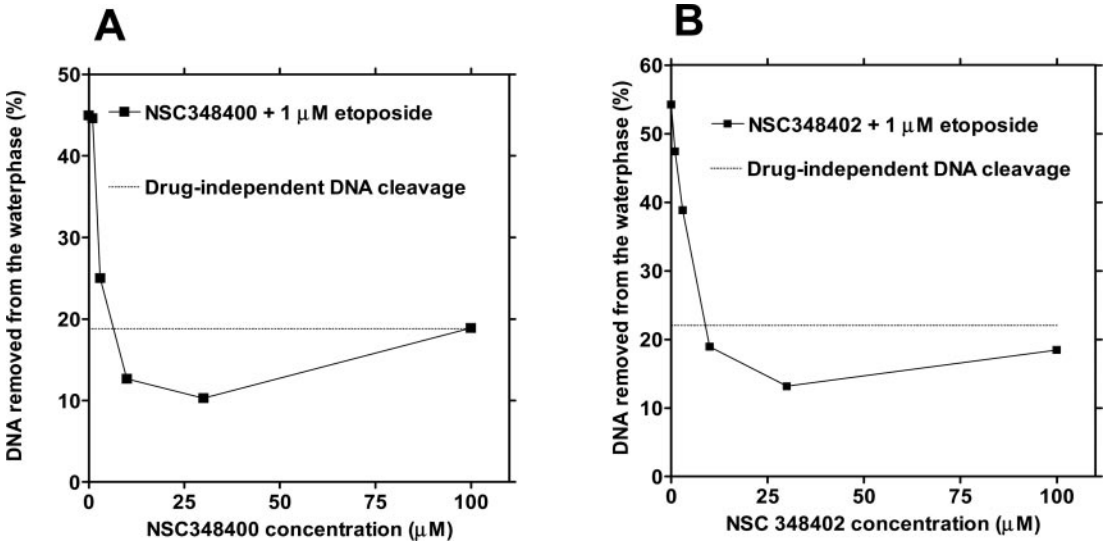

Fig. 7. NSC348400 (A) and NSC 348402 (B) antagonizes etoposide-induced increases at the level of topoisomerase IIα-DNA covalent complex formation. Purified topoisomerase IIα was incubated in the presence of 1 μM etoposide and increasing concentrations of the purine compounds. The level of topoisomerase IIα-DNA covalent complexes formed in the absence of any drug is depicted as dashed lines for comparison. Both compounds, as well as NSC348401 (data not shown), antagonized the effect of etoposide on increasing the level of topoisomerase IIα-DNA covalent complex formation.

persensitivity is unknown but may be due to defects in the ability of the mutant enzymes to catalyze DNA strand passage at low ATP levels (Wessel et al., 2002), leading to the purine analogs more efficiently competing out ATP binding.

Cross-Resistance Patterns within a Panel of Cell Lines Suggest That Topoisomerase IIα Is a Functional Cellular Target of the Most Potent Nonmetal Purine Analogs. One way to discriminate whether a putative drug target is functional in cells is to assess whether cell lines expressing different levels of that target display altered sensitivity toward the drug. We therefore tested the sensitivity of a small panel of small-cell lung cancer OC-NYH–derived cells against the three most potent nonmetal compounds, NSC348400, NSC348401, and NSC348402. OC-NYH is the parental cell line, OC-NYH/DOX has both topoisomerase IIα and topoisomerase IIβ down-regulated, OC-NYH/VM has topoisomerase IIα down-regulated, OC-NYH/pACR8 has topoisomerase IIβ down-regulated, and OC-NYH/DAU overexpresses MDR1. The latter cell line can be used to assess whether these purines are substrates for the P-glycoprotein pump. These cell lines have all been characterized (Rothenborg-Jensen et al., 2001). The result of this analysis is depicted in Fig. 8, A–C (OC-NYH/DAU data not included for clarity). Figure 8D shows the sensitivity of these cell lines toward etoposide. It can be seen that all cell lines except OC-NYH are highly resistant to etoposide. From Fig. 8, A–C, it can be seen that OC-NYH/DOX and OC-NYH/VM, the two cell lines with topoisomerase IIα down-regulated, are cross-resistant to these purines. Likewise, it has previously been shown that cells with reduced topoisomerase IIα levels are cross-resistant to the catalytic inhibitor ICRF-193 (Kobayashi et al., 2001; Adachi et al., 2003). On the other hand, OC-NYH/pACR8, in which only topoisomerase IIβ is down-regulated, was not cross-resistant to any significant extent with NSC348400 and NSC348401. Although this cell line seems to be cross-resistant toward NSC348402 at 1.0 μM, it was not at 2.0 μM. Together, these data suggest that topoisomerase IIα was a functional target for these purine ana-

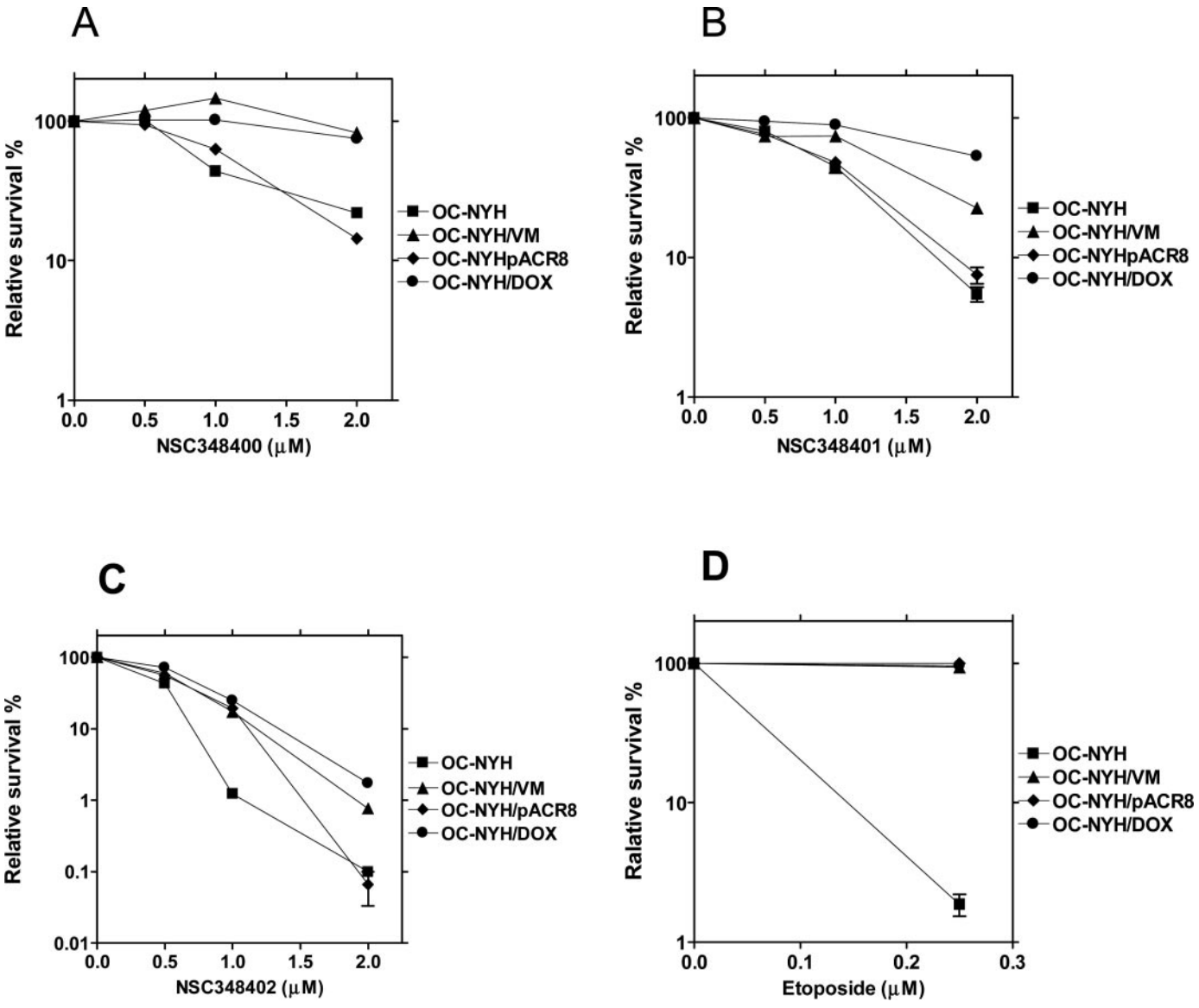

Fig. 8. Cross-resistance patterns of a panel of small cell lung cancer cells against NSC348400 (A), NSC348401 (B), and NSC348402 (C). The OC-NYH/DOX and OC-NYH/VM cell lines with reduced topoisomerase IIα expression were both resistant to these purine compounds, whereas the OC-NYH/pACR8 cell line with reduced topoisomerase IIβ expression was not resistant. Error bars represent S.E.M. of three different determinations.

logs in human cancer cells. It is noteworthy that OC-NYH/DAU cells overexpressing MDR1 were fully sensitive toward these compounds, suggesting that they do not have MDR1 liability. The reduced level of cross-resistance, compared with etoposide, may indicate that these purines have biological targets in addition to topoisomerase II.

Discussion

We previously identified NSC35866 as a catalytic inhibitor of topoisomerase IIα in vitro and showed that in cells it has the ability to modulate/antagonize the cytotoxicity and DNA strand breaks induced by etoposide (Jensen et al., 2005). In that study, NSC35866 was unique among a series of S^6-substituted purines (including 6-thiopurine, 6-thioguanine, azathioprine, 6-methylthioguanine, 2-thiopurine, and 2,6-dithiopurine) in being able to protect against etoposide-induced cytotoxicity in human cancer cells. However, the low potency of NSC35866 (30 μM in the ATPase assay and 750 μM in the DNA strand passage assay) precluded the use of this compound as a pharmacological modulator of etoposide because pronounced off-target effects would be likely at such high concentrations. It is noteworthy that some of the S^6-substituted compounds that were not capable of suppressing the effects of etoposide were highly potent catalytic inhibitors of topoisomerase IIα in vitro (Jensen et al., 2005). We therefore initiated the present study to determine whether we could identify more potent compounds similar to NSC35866 that could pharmacologically modulate the activity of etoposide. We used an enzyme-linked ATPase assay as a primary screen for potency against purified recombinant expressed human topoisomerase IIα. This approach was valid because the potency of 10 selected ATPase inhibitor correlated with their potency as inhibitors of the complete DNA strand passage (decatenation) reaction of this enzyme, which is the more pharmacologically relevant activity of topoisomerase II. When assessed in an assay that measured the levels of topoisomerase IIα-DNA covalent complexes, none of the 40 purine analogs was found to increase the level of these complexes to any great extent, compared with etoposide which confirmed that these purine analogs are catalytic topoisomerase IIα inhibitors.

To further define the structural factors that resulted in high ATPase inhibitory potency for the purines and the purine-like compounds 3D-QSAR CoMFA and CoMSIA analyses were carried out to derive models for the prediction of activity to aid in the design and synthesis of new more active analogs. Based on a common substructure alignment (Fig. 1B), both CoMFA and CoMSIA analyses gave high quality models based on their q^2 values (Table 2). The largest contributions to the CoMSIA field were hydrophobic and hydrogen bond donor contributions, in that order. Mapping of these fields onto the structure of NSC348400, a potent purine analog (Figs. 4 and 5), showed that favorable hydrophobic contributions to the ATPase inhibitory activity of these compounds were localized in the region around the aromatic groups bonded to the sulfur ether atom. Both hydrogens of the amino group substituent on the purine ring were also highly favored as hydrogen bond donors. The CoMSIA electrostatic field also showed that polar substituent such as nitro and the benzoxadiazol groups were also favored. Steric fields in both models showed that a methylene group bonded to the sulfur ether atom was not favored. As shown in Fig. 1B, this was probably due to the flexibility of the methylene linking group allowing the purine and aromatic rings to assume a nearly coplanar configuration.

NSC35866 was previously shown to protect human cancer cells against the effects of the topoisomerase II poison etoposide (Jensen et al., 2005). However, this was not the case for the NSC348400, NSC348401, or the NSC348402 compounds. This was an unexpected result given that these compounds antagonized the effect of etoposide on topoisomerase IIα-DNA covalent complex formation with purified topoisomerase IIα. We can envisage several possible explanations for this observation. It may be that these purine compounds were not sufficiently cell-permeable for a 20-min incubation to give inhibitory levels of the drug. NSC348400, in particular, with its sugar residue, would not be very lipophilic, and both NSC348401 and NSC348402 have polar substituents that could reduce their lipophilicity. Second, the molecular interaction of NSC348400, NSC348401, and the NSC348402 with topoisomerase IIα may be different from that of NSC35866. Although NSC35866, NSC348400, NSC348401, and NSC348402 are all catalytic topoisomerase IIα inhibitors, subtle differences in their mode of interaction with topoisomerase IIα may exist. For instance, one important difference between NSC348400, NSC348401 and NSC348402, and NSC35866 is the presence of polar substituents at the S^6-substituted moiety, which may alter the mode and/or site of interaction with topoisomerase II. The fact that the expression levels of topoisomerase IIα in cells correlates with cytotoxicity of NSC348400, NSC348401, and NSC348402 in the clonogenic assays suggested that topoisomerase IIα was a functional cellular target in mediating the cellular effects of these compounds, a conclusion that would favor the second hypothesis.

It is also interesting to note that these compounds are not MDR1 substrates. Thus, these compounds may be useful as topoisomerase II-targeted anticancer agents on their own. Our 3D-QSAR models will allow us, within the chemical space that we explored, to design compounds in silico that are even more potent catalytic inhibitors of topoisomerase II.

Acknowledgments

Dr. John L. Nitiss (St. Jude Children's Research Hospital, Memphis, TN) is acknowledged for providing DNA construct and yeast strain for the overexpressing of human topoisomerase IIα in yeast. The technical assistance of Sanne Christiansen, Annette Nielsen, and Mette Christiansen at TopoTarget A/S in performing decatenation assays and clonogenic assays is likewise acknowledged.

References

Adachi N, Suzuki H, Iiizumi S, and Koyama H (2003) Hypersensitivity of nonhomologous DNA end-joining mutants to VP-16 and ICRF-193: implications for the repair of topoisomerase II-mediated DNA damage. *J Biol Chem* **278:**35897–35902.

Akimitsu N, Adachi N, Hirai H, Hossain MS, Hamamoto H, Kobayashi M, Aratani Y, Koyama H, and Sekimizu K (2003) Enforced cytokinesis without complete nuclear division in embryonic cells depleting the activity of DNA topoisomerase IIα. *Genes Cells* **8:**393–402.

Andoh T and Ishida R (1998) Catalytic inhibitors of topoisomerase II. *Biochim Biophys Acta* **1400:**155–171.

Baldwin EL, Byl JA, and Osheroff N (2004) Cobalt enhances DNA cleavage mediated by human topoisomerase II alpha in vitro and in cultured cells. *Biochemistry* **43:**728–735.

Classen S, Olland S, and Berger JM (2003a) Structure of the topoisomerase II ATPase region and its mechanism of inhibition by the chemotherapeutic agent ICRF-187 [published erratum appears in *Proc Natl Acad Sci USA* **100:**14510, 2003]. *Proc Natl Acad Sci USA* **100:**10629–10634.

Cramer RD III, Patterson DE, and Bunce JD (1988) Comparative molecular field

analysis (CoMFA). 1. Effect of shape on binding of steroids to carrier proteins. *J Am Chem Soc* **110:**5959–5967.
Hasinoff BB, Wu X, Begleiter A, Guziec L, Guziec F, Giorgianni A, Yang S, Jiang Y, and Yalowich JC (2006) Structure-activity study of the interaction of bioreductive benzoquinone alkylating agents with DNA topoisomerase II. *Cancer Chemother Pharmacol* **57:**221–233.
Hasinoff BB, Wu X, Krokhin OV, Ens W, Standing KG, Nitiss JL, Sivaram T, Giorgianni A, Yang S, Jiang Y, et al. (2005) Biochemical and proteomics approaches to characterize topoisomerase IIα cysteines and DNA as targets responsible for cisplatin-induced inhibition of topoisomerase IIα. *Mol Pharmacol* **67:**937–947.
Hofland KF, Thougaard AV, Dejligbjerg M, Jensen LH, Kristjansen PE, Rengtved P, Sehested M, and Jensen PB (2005) Combining etoposide and dexrazoxane synergizes with radiotherapy and improves survival in mice with central nervous system tumors. *Clin Cancer Res* **11:**6722–6729.
Holm B, Sehested M, and Jensen PB (1998) Improved targeting of brain tumors using dexrazoxane rescue of topoisomerase II combined with supralethal doses of etoposide and teniposide. *Clin Cancer Res* **4:**1367–1373.
Holm C, Goto T, Wang JC, and Botstein D (1985) DNA topoisomerase II is required at the time of mitosis in yeast. *Cell* **41:**553–563.
Jensen LH, Renodon-Corniere A, Wessel I, Langer SW, Sokilde B, Carstensen EV, Sehested M, and Jensen PB (2002) Maleimide is a potent inhibitor of topoisomerase II in vitro and in vivo: a new mode of catalytic inhibition. *Mol Pharmacol* **61:**1235–1243.
Jensen LH, Thougaard AV, Grauslund M, Sokilde B, Carstensen EV, Dvinge HK, Scudiero DA, Jensen PB, Shoemaker RH, and Sehested M (2005) Substituted purine analogues define a novel structural class of catalytic topoisomerase II inhibitors. *Cancer Res* **65:**7470–7477.
Jensen PB, Christensen IJ, Sehested M, Hansen HH, and Vindelov L (1993) Differential cytotoxicity of 19 anticancer agents in wild type and etoposide resistant small cell lung cancer cell lines. *Br J Cancer* **67:**311–320.
Jensen PB and Sehested M (1997) DNA topoisomerase II rescue by catalytic inhibitors: a new strategy to improve the antitumor selectivity of etoposide. *Biochem Pharmacol* **54:**755–759.
Klebe G, Abraham U, and Mietzner T (1994) Molecular similarity indices in a comparative analysis (CoMSIA) of drug molecules to correlate and predict their biological activity. *J Med Chem* **37:**4130–4146.
Kobayashi M, Adachi N, Aratani Y, Kikuchi A, and Koyama H (2001) Decreased topoisomerase IIα expression confers increased resistance to ICRF-193 as well as VP-16 in mouse embryonic stem cells. *Cancer Lett* **166:**71–77.
Kohn KW and Grimek-Ewig RA (1973) Alkaline elution analysis, a new approach to the study of DNA single-strand interruptions in cells. *Cancer Res* **33:**1849–1853.
Kubinyi H, Hamprecht FA, and Mietzner T (1998) Three-dimensional quantitative similarity-activity relationships (3D QSiAR) from SEAL similarity matrices. *J Med Chem* **41:**2553–2564.
Larsen AK, Escargueil AE, and Skladanowski A (2003) Catalytic topoisomerase II inhibitors in cancer therapy. *Pharmacol Ther* **99:**167–181.
Lindsley JE (2001) Use of a real-time, coupled assay to measure the ATPase activity of DNA topoisomerase II. *Methods Mol Biol* **95:**57–64.
Morris SK, Baird CL, and Lindsley JE (2000) Steady-state and rapid kinetic analysis of topoisomerase II trapped as the closed-clamp intermediate by ICRF-193. *J Biol Chem* **275:**2613–2618.
Rothenborg-Jensen L, Hansen HF, Wessel I, Nitiss JL, Schmidt G, Jensen PB, Sehested M, and Jensen LH (2001) Linker length in podophyllotoxin-acridine conjugates determines potency in vivo and in vitro as well as specificity against MDR cell lines. *Anticancer Drug Des* **16:**305–315.
Sehested M and Jensen PB (1996) Mapping of DNA topoisomerase II poisons (etoposide and clerocidin) and catalytic inhibitors (aclarubicin, ICRF-187) to four distinct steps in the topoisomerase II catalytic cycle. *Biochem Pharmacol* **51:**879–886.
Sehested M, Jensen PB, Sorensen BS, Holm B, Friche E, and Demant EJF (1993) Antagonistic effect of the cardioprotector (+)-1,2-bis(3,5-dioxopiperazinyl-1-yl)propane (ICRF-187) on DNA breaks and cytotoxicity induced by the topoisomerase II directed drugs daunorubicin and etoposide (VP-16). *Biochem Pharmacol* **46:**389–393.
Wang H, Mao Y, Chen AY, Zhou N, LaVoie EJ, and Liu LF (2001) Stimulation of topoisomerase II-mediated DNA damage via a mechanism involving protein thiolation. *Biochemistry* **40:**3316–3323.
Wang JC (2002) Cellular roles of DNA topoisomerases: a molecular perspective. *Nat Rev Mol Cell Biol* **3:**430–440.
Wessel I, Jensen LH, Renodon-Corniere A, Sorensen TK, Nitiss JL, Jensen PB, and Sehested M (2002) Human small cell lung cancer NYH cells resistant to the bisdioxopiperazine ICRF-187 exhibit a functional dominant Tyr165Ser mutation in the Walker A ATP binding site of topoisomerase IIα. *FEBS Lett* **520:**161–166.
Wilstermann AM and Osheroff N (2003) Stabilization of eukaryotic topoisomerase II-DNA cleavage complexes. *Curr Top Med Chem* **3:**321–338.
Yang X, Li W, Prescott ED, Burden SJ, and Wang JC (2000) DNA topoisomerase IIβ and neural development. *Science (Wash DC)* **287:**131–134.
Zhang H, D'Arpa P, and Liu LF (1990) A model for tumor cell killing by topoisomerase poisons. *Cancer Cells* **2:**23–27.
Zhou N, Xiao H, Li TK, Nur EKA, and Liu LF (2003) DNA damage-mediated apoptosis induced by selenium compounds. *J Biol Chem* **278:**29532–29537.

Address correspondence to: Dr. Brian Hasinoff, Faculty of Pharmacy, University of Manitoba, Winnipeg, Manitoba R3T 2N2, Canada. E-mail: b_hasinoff@umanitoba.ca